Proceedings of the ASME 2010 3rd Joint US-European Fluids Engineering Summer Meeting and 8th International Conference on Nanochannels, Microchannels, and Minichannels
FEDSM-ICNMM2010
August 1-5, 2010, Montreal, Canada

FEDSM-ICNMM2010-30619

COMPUTATION OF AN UNSTEADY ORIFICE FLOW IN A CIRCULAR PIPE FROM WALL PRESSURE MEASUREMENTS BASED ON MEASUREMENT-INTEGRATED SIMULATION USING A TURBULENT MODEL

Mitsuhiro Nakao
Tokyo Institute of Technology
Yokohama, JAPAN

Kenji Kawashima
Tokyo Institute of Technology
Yokohama, JAPAN

Toshiharu Kagawa
Tokyo Institute of Technology
Yokohama, JAPAN

ABSTRACT

Visualizing the state of real turbulent flow is important in many applications such as safe operation and fault diagnosis in plant or pipeline. Two approaches to this purpose exist: experimental measurement and numerical simulation. In experimental measurement, reliability of the result at measured point is easy to evaluate. However, information of the whole flow field is difficult to obtain. On the other hand, numerical simulation easily obtains any information of the flow field. However, the reliability of the result strongly depends on the numerical model and boundary condition and/or the initial condition. In general, the more precise results are needed, the heavier computation load we spend. None of these approaches is superior, and combination methods of them are subjected to extensive research. Above all, we particularly paid attention to measurement-integrated (MI) simulation proposed by Hayase et al. MI simulation can expect to reduce computational load.

We have applied MI simulation to unsteady oscillatory airflows passing through an orifice. In our previous study, a standard k-ε model was used for MI simulation. Estimation error remained due to inadequate consideration of the feedback law. In our latest study, the feedback law was decided considering an effect of computation grid on CFD of contracted flow. As a result, wall pressures near the orifice plate and axial velocities on vena contracta estimated with MI simulation showed good agreement with that of measurement.

In the present paper, we deal with visualization of unsteady oscillatory airflows passing through an orifice from wall pressure measurement based on MI simulation using a turbulent model. The former studies have used measured inlet flow rate which is unknown in many actual case. Compared with the flow rate measurement, wall pressure measurement is simple. Therefore, we consider MI simulation using only wall pressure are of practical use. The developed MI simulation was performed with unsteady flow rate with the frequency up to 10 Hz. Computation results obtained with the developed MI simulation using coarse computation grid is compared with experimental results. It is confirmed that flow field obtained with the developed MI simulation is close to that of experiment.

INTRODUCTION

Visualizing the state of real turbulent flow is important in many applications such as safe operation and fault diagnosis in plant or pipeline.

The methods used to visualize the flow conditions can be classified into two approaches. One is experimental measurement, and the other is numerical simulation by solving several equations. Experimental measurement methods include the use of velocity and pressure sensors and visualization techniques such as particle image velocimetry and particle tracking velocimetry. Flow conditions can be accurately obtained at measured points by using sensors. However, sensors are not suitable for obtaining velocity profiles or pressure distributions. By contrast, visualization techniques are able to obtain these distributions. However, the available flow field is limited because particle behavior is tracked using a laser and a camera. In contrast, simulation can easily obtain a flow field. However, a long computation time is needed to obtain good results, especially under turbulent conditions. None of these approaches is superior, and combination methods of them are subjected to extensive research.

We have focused on measurement-integrated (MI) simulation, which was first proposed by Hayase et al **[1]**. MI simulation is a kind of observer that employs a CFD scheme as the mathematical model for the relevant system. The block diagram in **Fig. 1** illustrates the concept of MI simulation. As a general rule for an observer, errors in the mathematical model will not affect the MI simulation results, since the difference

between the computation and measurement results is fed back to the model through the feedback law. This allows us to use a simple model in CFD schemes, such as one that has a coarse computational grid or a turbulent model that is easy to apply. Consequently, using an MI simulation is expected to reduce the computational load. The effectiveness of MI simulations has been demonstrated in several applications, including the Karman vortex street behind a square cylinder **[2]**, blood flow in the aneurysmal aorta **[3]**, and the reproduction of fluctuating turbulent flow in a square duct **[1]**.

We have applied MI simulation to unsteady oscillatory airflows passing through an orifice flow. In our previous study, a standard k-ε model was used for MI simulation **[4]**. Estimation error was remained due to inadequate consideration of feedback law. In our latest study, the feedback law was decided considering an effect of computation grid on CFD of contracted flow **[5]**. As a result, wall pressures near the orifice plate and axial velocities on vena contracta estimated with MI simulation showed good agreement with that of measurement.

In the present paper, we deal with visualization of unsteady oscillatory airflows passing an orifice flow from wall pressure measurement based on MI simulation using turbulent model. The former studies **[4, 5]** have used measured inlet flow rate which is unknown in many actual case. Compared with the flow rate measurement, wall pressure measurement is simple. Therefore, we consider MI simulation using only wall pressure are of practical use. We confirmed the effectiveness of the MI simulation in flow field with constant inlet flow rate **[6]**. In this paper, the developed MI simulation was performed with unsteady flow rate with the frequency up to 10 Hz. Computation results obtained with the developed MI simulation using coarse computation grid is compared with experimental results. It is confirmed that flow field obtained with the developed MI simulation is close to that of experiment.

NOMENCLATURE

e : normalized error [-]
f : feedback signal adding to vena contracta [-]
k : normalized turbulent kinetic energy $k=\hat{k}/U_0^2$ [-]
KP_U : proportional gain of feedback signal Δu_0 [-]
KI_U : integral gain of feedback signal Δu_0 [-]
KP_P : proportional gain of feedback signal f [-]
KI_P : integral gain of feedback signal f [-]
p : normalized pressure $p=P/\rho U_0^2$ [-]
P : pressure [Pa]
P_1 : upstream pressure of the orifice [Pa]
P_2 : downstream pressure of the orifice [Pa]
ΔP : differential pressure of the orifice plate [-]
Q : volumetric flow rate [m^3/s]
r : normalized radial coordinate $r=R/R_0$ [-]
R : radial coordinate [m]
R_0 : pipe radius [m]
t : time [s]
u : normalized axial velocity $u = U/U_0$ [-]

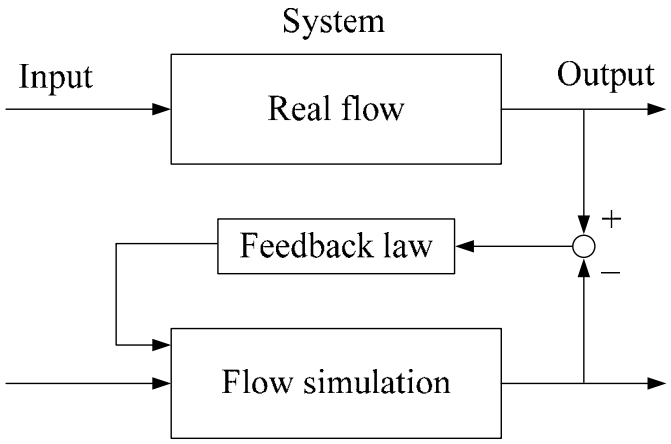

Figure 1. Concept of MI simulation

U : axial velocity [m/s]
U_0 : average axial velocity at inlet of the pipe [m/s]
Δu_0 : feedback signal to control inlet velocity [-]
v : normalized radial velocity $v=\hat{v}/U_0$ [-]
x : normalized axial coordinate $x=\hat{x}/R_0$ [-]
X : distance from the orifice [m]

α : contraction coefficient [-]
β : beta ratio [-]
ε : normalized dissipation ratio $\varepsilon=\varepsilon R_0/U_0^3$ [-]
θ : temperature of air [K]
ρ : density [kg/m^3]
μ : viscosity [Pa·s]
ν_t : normalized turbulent kinetic viscosity $\nu_t=\hat{\nu}_t/R_0U_0$ [-]
ν_{eff} : normalized effective kinetic viscosity
$\nu_{eff}=\mu/\rho+\nu_t$ [-]
C_1, C_2 , C_μ, σ_k, σ_τ:model constants of standard k-ε model

subscript
* : Estimated value
^ : Dimensional value
’ : Correction value in SIMPLE method
exp: Measured value
sim: Calculated value

NUMERICAL MODELLING

The axisymmetric one-hole plate in **Figure 2** was modeled in two dimensions. Both pressures and velocities around the orifice have earlier been measured and were used to anchor the calculation.

These measurements were carried out in a 53 mm diameter smooth pipe rig. The plate consists of a concentric hole with a diameter of 31 mm, giving a β ratio of 0.6. The plate is 2 mm thick.

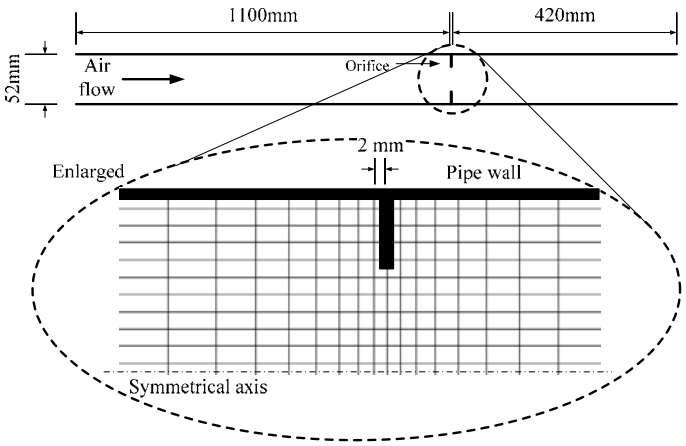

Figure 2. Target flow field and computational grid around an orifice

An actual orifice plate has edge around the concentric hole. In general, much computation grids are needed around an edge for accurate computation. Large number of computation causes large computation time. Therefore, we assume the orifice plate as a restriction to achieve short computation time, expecting a feedback effect to correct flow field.

Staggered grid system is employed for stable computations. Grid spacing in radial direction is constant at 2.6 mm. In axial direction, grid spacing around the orifice plate is 2 mm, and increased by 1.2 times.

FORMULATION

The governing equations for the flow in a pipeline considered in this simulation are the non-dimensional Navier-Stokes equations expressed in cylindrical coordinates; they include a feedback term and the equation of continuity and are given as follows:

$$\frac{\partial u}{\partial t}+u\frac{\partial u}{\partial x}+v\frac{1}{r}\frac{\partial(ru)}{\partial r}=-\frac{\partial p}{\partial x}+\nu_{\text{eff}}\left\{\frac{\partial^2 u}{\partial x^2}+\frac{1}{r}\frac{\partial}{\partial r}\left(r\frac{\partial u}{\partial r}\right)+\frac{\partial^2 u}{\partial x^2}+\frac{1}{r}\frac{\partial}{\partial r}\left(r\frac{\partial v}{\partial x}\right)\right\}+f, \quad (1)$$

$$\frac{\partial v}{\partial t}+u\frac{\partial v}{\partial x}+v\frac{1}{r}\frac{\partial(rv)}{\partial r}=-\frac{\partial p}{\partial r}+\nu_{\text{eff}}\left\{\frac{\partial^2 v}{\partial x^2}+\frac{1}{r}\frac{\partial}{\partial r}\left(r\frac{\partial v}{\partial r}\right)+\frac{\partial}{\partial x}\left(\frac{\partial u}{\partial r}\right)+\frac{1}{r}\frac{\partial}{\partial r}\left(r\frac{\partial v}{\partial r}\right)-2\frac{v}{r^2}\right\}, \quad (2)$$

$$\frac{\partial u}{\partial x}+\frac{1}{r}\frac{\partial(rv)}{\partial r}=0. \quad (3)$$

The last term in Eq. (1) f represents the feedback value. The transport equations for k and ε are given as:

$$\frac{\partial k}{\partial t}+u\frac{\partial k}{\partial x}+v\frac{1}{r}\frac{\partial(rk)}{\partial r}=\frac{\nu_{\text{eff}}}{\sigma_k}\left\{\frac{\partial}{\partial x}\left(\frac{\partial k}{\partial x}\right)+\frac{1}{r}\frac{\partial}{\partial r}\left(r\frac{\partial k}{\partial r}\right)\right\}+2\nu_t\left\{\left(\frac{\partial u}{\partial x}\right)^2+\left(\frac{\partial v}{\partial r}\right)^2+\frac{1}{2}\left(\frac{\partial u}{\partial r}+\frac{\partial v}{\partial x}\right)^2\right\}-\varepsilon, \quad (4)$$

$$\frac{\partial \varepsilon}{\partial t}+u\frac{\partial \varepsilon}{\partial x}+v\frac{1}{r}\frac{\partial(r\varepsilon)}{\partial r}=\frac{\nu_{\text{eff}}}{\sigma_\varepsilon}\left\{\frac{\partial}{\partial x}\left(\frac{\partial \varepsilon}{\partial x}\right)+\frac{1}{r}\frac{\partial}{\partial r}\left(r\frac{\partial \varepsilon}{\partial r}\right)\right\}+C_1G\frac{\varepsilon}{k}-C_2\frac{\varepsilon^2}{k}. \quad (5)$$

The model constants are selected as follows: $\sigma_k = 1.0$ $\sigma_\varepsilon = 1.3$ $C_1 = 1.44$ $C_2 = 1.92$ $C_\mu = 0.09$. The temperature and physical properties of air were treated as constants ($\theta = 291$ K, $\rho = 1.21$ kg/m^3, $\mu = 1.8\times10^{-5}$ Pa·s).

As the initial conditions, a uniform velocity equivalent to a Reynolds number of 3000 is assumed at the inlet boundary and an atmospheric pressure is assumed at the downstream boundary of the pipeline.

At the upstream domain boundary, a uniform average axial velocity is imposed, whereas at the downstream boundary, the axial velocity gradient is assumed to be 0.

Fine computational grids are generally required for computing flow in a viscous sublayer near a pipeline wall since there is a large velocity gradient in turbulent flow. For efficient computation, the wall functions are employed to reduce the number of the computational grid. To avoid performing computations in the viscous sublayer, the first grid node is considered to lie outside the viscous sublayer. The wall functions are used to form a bridge between the wall conditions and the first grid node. This enables near-wall boundary conditions for the mean flow and turbulence transport equations to be determined. In this paper, a log law was used for the wall. The wall boundary condition was specified by the following wall function **[7]**:

$$\frac{U_P}{(\tau/\rho)}C_\mu^{\frac{1}{4}}k_p^{\frac{1}{2}}=\frac{1}{\kappa}\ln\left(EY\frac{C_\mu^{\frac{1}{4}}k_p^{\frac{1}{2}}}{\nu}\right). \quad (6)$$

Here, U_P and k_p are the velocity and turbulent kinetic energy at a node near the wall, respectively. Y is the distance from the wall, τ is the shear stress on the wall, and ν is the kinetic viscosity. Values of 0.41 and 9.7 are assigned to the von Karman constant κ and the constant E, respectively.

COMPENSATATION OF COMPUTATIONAL ACCURACY IN COARSE GRID

The Following equation gives relation between flow rate through an orifice plate and differential pressure of the orifice;

$$Q=\frac{\alpha}{\sqrt{1-\beta^4}}\pi(R_0\beta)^2\sqrt{\frac{2\Delta P}{\rho}} \quad (7)$$

However, CFD with a coarse grid gives lower estimation of differential pressure caused by an orifice plate **[8]**. From consideration based on Eq. (7), this means that contraction

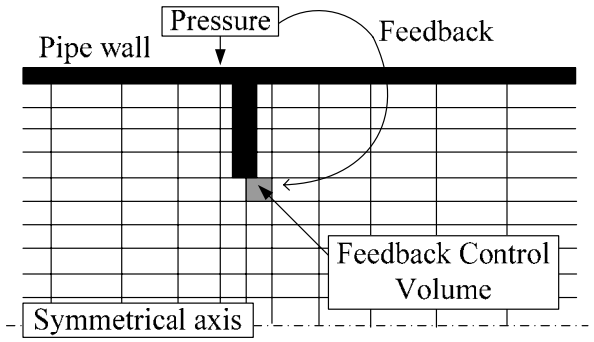

Figure 3. Feedback added to the vena contracta

coefficient α is estimated larger than actual value.

Therefore, we compensate for the estimation error by adding a feedback signal. In our previous study **[5]**, the error in P_1 between the measured and calculated values is defined in dimensionless form as follows:

$$e_1 = \frac{P_{1,\exp}}{\rho U_0{}^2} - p_{1,\sim} \tag{8}$$

The feedback signal f is defined as

$$f = -KP_{\mathrm{p}}\left(e_1 + \sum e_1 \Big/ KI_{\mathrm{p}}\right) \tag{9}$$

A proportional plus integral (PI) controller, which is widely used in industrial process control, is employed as shown in Eq. (8). This feedback signal f is added to the control volume, as shown in **Fig. 3**. A conventional CFD that does not include f cannot produce results close to those of real flow using such a coarse computational grid.

ESTIMATION OF INLET VELOCITY

The differential pressure across the orifice $\Delta P_{\sim}$ is controlled by adjusting the inlet velocity. The error in $\Delta P_{\sim}$ between the measured and calculated values is defined in the same manner as for e_2 as in Eq. (9).

$$e_2 = \sqrt{\Delta P_{\exp} \Big/ \left(\rho U_0{}^2\right)} - \sqrt{\Delta p_{\sim}} \ . \tag{10}$$

In this feedback, the proportional gain KP_{U} must be normalized since the inlet velocity is used for nondimensionalization. Therefore, the following equations are expressed in dimensional form.

The inlet velocity increment at a certain stage of the calculation can be described using a constant proportional gain K as follows:

$$\Delta U_0 = K\left(\sqrt{\Delta P_{\exp}} - \sqrt{\Delta P_{\sim}}\right). \tag{11}$$

For a certain constant a, the following equality holds in convergent calculations:

$$U_{0,\exp} = a\sqrt{\Delta P_{2,\exp}} \ . \tag{12}$$

Dividing both sides of the equation, gives the following equation:

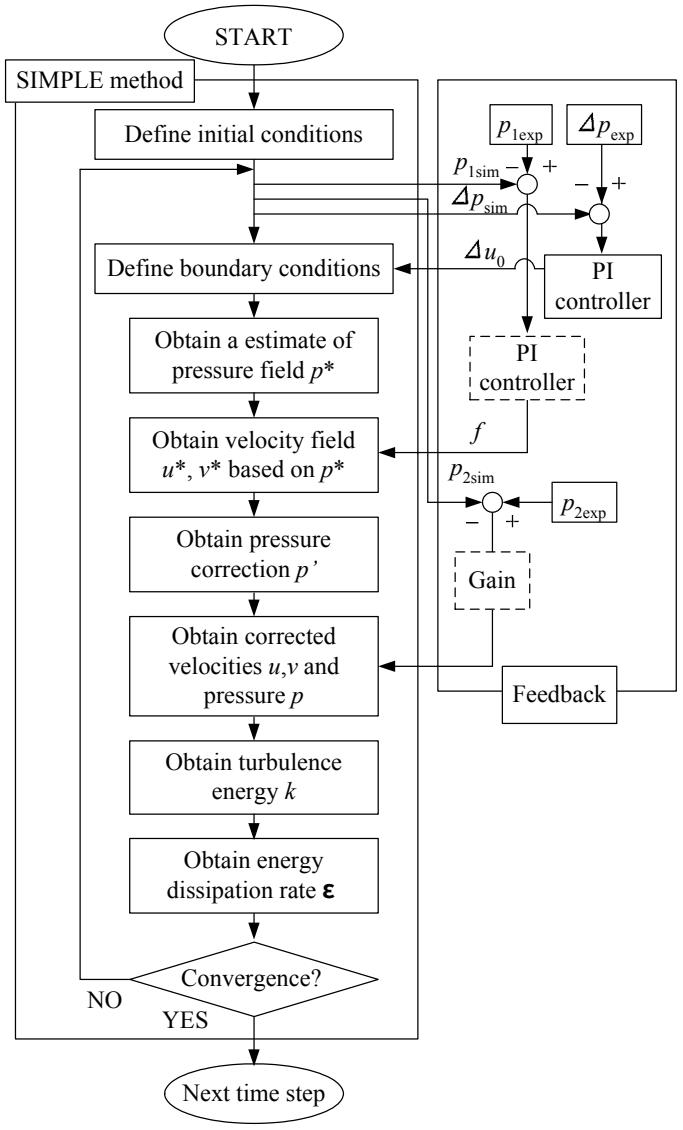

Figure 4. Computation flow chart

$$\frac{\Delta U_0}{U_{0,\exp}} = \frac{K}{a\sqrt{\Delta P_{\exp}}}\left(\sqrt{\Delta P_{\exp}} - \sqrt{\Delta P_{\sim}}\right). \tag{13}$$

The left-hand side of Eq. (13) gives the nondimensional response and it must be constant for any inlet flow rate. If the computation has converged, nondimensionalization using the inlet velocity will be valid. The nondimensional differential pressure ΔP will then be independent of the inlet flow rate.

Therefore, the term in parentheses in Eq. (13) will be a constant, so that the proportional gain can be described as:

$$\frac{K}{\sqrt{\Delta P_{\exp}}} = KP_{\mathrm{U}} = const. \ . \tag{14}$$

The feedback signal added to the inlet velocity is given in nondimensional form as follows:

$$\Delta u_0 = KP_{\mathrm{U}}\sqrt{\Delta P_{\exp}}\left(e_2 + \sum e_2 \Big/ KI_{\mathrm{U}}\right). \tag{15}$$

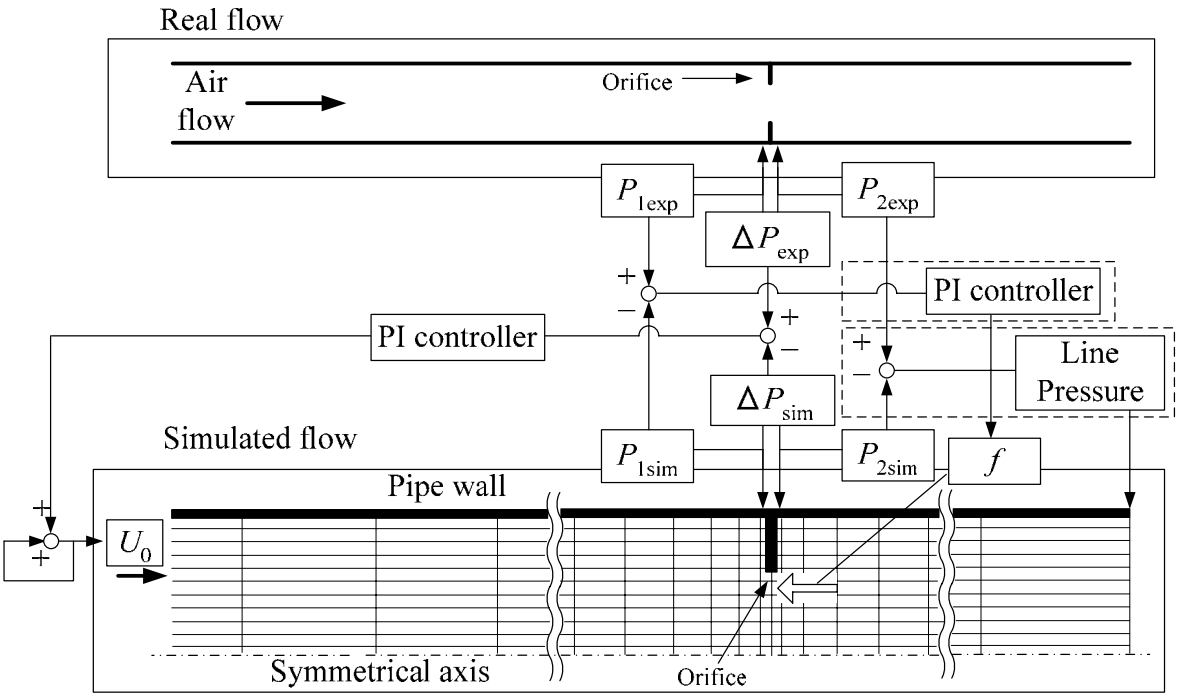

Figure 5. Apparatus of developed MI simulation

FEEDBACK LAW

The procedure of the computation is shown in **Fig. 4**. In addition to the ordinary procedure of the SIMPLE **[9]**, feedback loops are added.

Figure 5 shows the apparatus used for the developed MI simulation. The computed flow field that corresponds to the real flow field is constructed on a computer. The upstream pressure P_1 and the downstream pressure P_2 are measured for the MI simulation. **Figure 5** shows the computation procedure of the proposed MI simulation. The proposed MI simulation uses three feedback loops: feedback control of the upstream pressure $P_{1,\mathrm{sim}}$, feedback control of the differential pressure ΔP_{sim} and line pressure.

The upstream pressure $P_{1,\mathrm{sim}}$ and the differential pressure ΔP_{sim} are controlled by PI controllers as outlined in the former chapters.

The line pressure is controlled by a P controller with the feedback signal shown in Eq. (16), which calculates the error between the measured upstream pressure $P_{2,\mathrm{exp}}$ and the computed upstream pressure $P_{2,\mathrm{sim}}$ as shown in Eq. (9).

$$\Delta p_{\mathrm{line}} = -\left(p_{2,\mathrm{exp}} - p_{2,\mathrm{sim}}\right) \qquad (16)$$

This feedback algorithm showed good results in steady condition. However, in unsteady condition, a computation with this feedback algorithm diverged. Therefore, feedback signal f in unsteady condition is assumed to be constant of the value obtained in the first time step of the computation.

An immense over shoot phenomenon which brings longer computation time and unstable computation is caused when all feedback valuables are added from beginning of the computation. Therefore, feedback procedure is separated to four steps as described in the chapter of results and discussion.

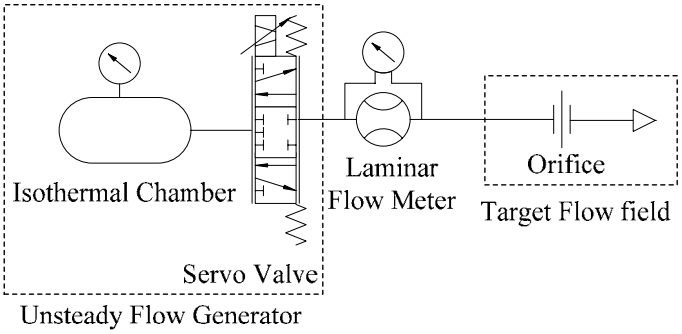

Figure 6. Experimental apparatus

EXPERIMENTAL SETUP

Figure 6 shows the experimental apparatus for unsteady flow experiments. The unsteady mass flow is generated using an isothermal chamber and a servo valve, as shown in **Fig. 6 [10]**. A quick response flow sensor is used for the flow rate measurement **[11]**. The inlet flow rate was a sinusoidal oscillatory flow with an average flow rate of 8.5×10^{-3} $\mathrm{m^3/s}$, amplitude of 1.7×10^{-3} $\mathrm{m^3/s}$, and frequencies of 0.5 Hz to 10 Hz. A low-pass filter was used to process the measured data; the cut-off frequency of the filter was set at twice the generated frequency. Filtered data were used for feedback.

Figure 7 shows the measurement points. Wall pressures point A to E and velocities on the center line of the pipe line

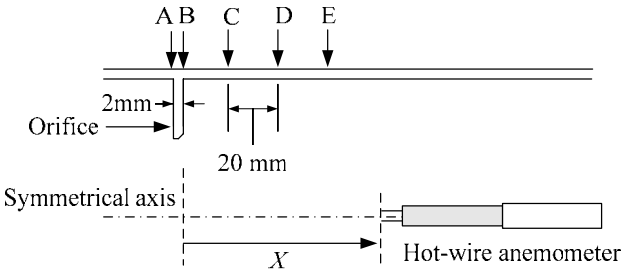

Figure 7. Measurement points

Table 1. Feedback gains

	KP_U	KI_U	KP_P	KI_P
STEP 1 (Initial)	0	0	0	0
STEP 2 ($\sum p' < 100$)	0.0019	0	0	0
STEP 3 ($\sum p' < 10$)	0.0019	0	4	9
STEP 4 ($\sum p' < 1$)	0.0019	10	4	9

were measured early. A pressure at point A is P_1, and a pressure at point B is P_2. Only these two pressures were used for feedback.

RESULTS AND DISCUSSIONS

The effectiveness of the developed MI simulation in steady turbulent flow is confirmed in our former study. The computation without the feedback with the computation grid shown in Fig. 2 estimates differential pressure caused by the orifice about 40% lower.

In this chapter, computation results of the MI simulation are compared to that of experiment in unsteady oscillatory condition. Feedback gains are configured by trial and error as shown in **Table 1**. The feedback gains are switched to next step values when the summation of correction pressures are less than a certain value.

Figure 8 shows the comparisons of upstream pressure P_1, downstream pressure P_2 and center velocity at X = 40 mm between the MI simulation and the experiment in sinusoidally oscillating flow rate with the frequency of 10 Hz. In principle, no steady-state error of a controlled value remains in a feedback control with PI controller. As shown in **Fig. 8**, controlled values of upstream pressure P_1 and downstream pressure P_2 are the same values with that of the experiment. On the other hand, computation of velocity at X = 40 mm is no controlled directly. Although, a computation result of the velocity has minimal error. **Figure 9** compares velocities at X = 40 mm with the frequencies up to 8 Hz, and shows excellent agreement. The validity of the developed MI simulation in sinusoidally oscillating condition up to 10 Hz was confirmed.

CLARIFIED PROBLEM

However, new issues are risen. In feedback control of line pressure, a deviation between computed P_2 and measured P_2 is added to all computation grids. This caused a problem of

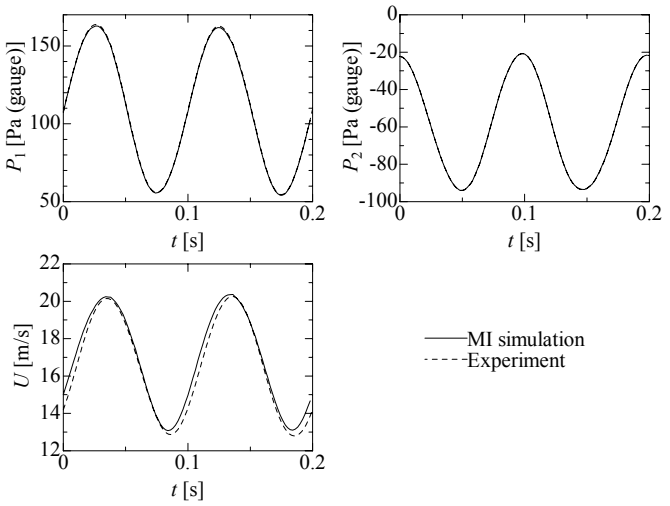

Figure 8. Comparisons of P_1, P_2 and velocity at X = 40 mm with the frequency of 10 Hz between experiment and the developed MI simulation

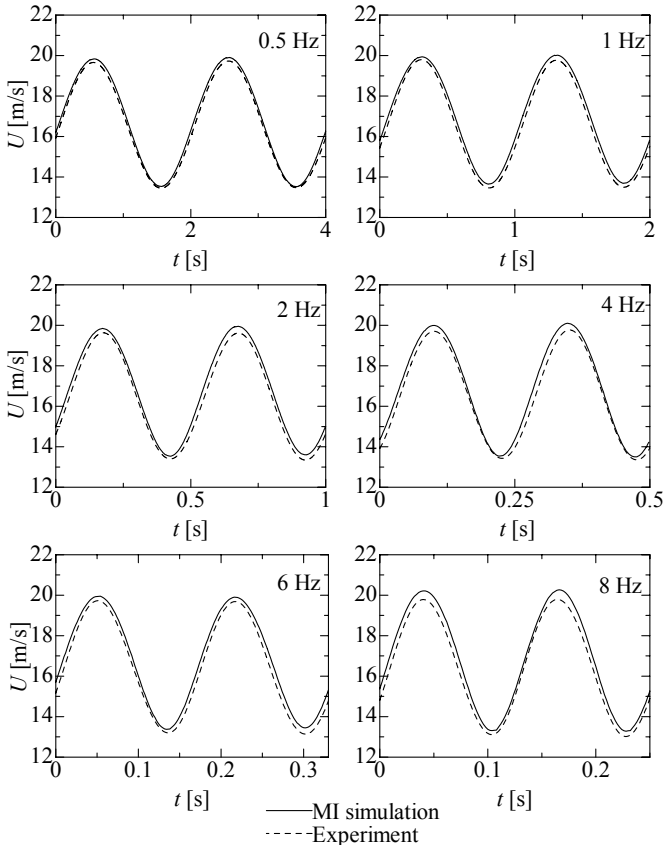

Figure 9. Comparisons of velocity at X = 40 mm up to 8 Hz between experiment and the developed MI simulation

consistency with other feedback controls. As a result, convergent solutions are affected by the settings of feedback gains. **Figure 10** shows variation of estimation of Q and feedback signal f against KP_U. Other feedback gains are the

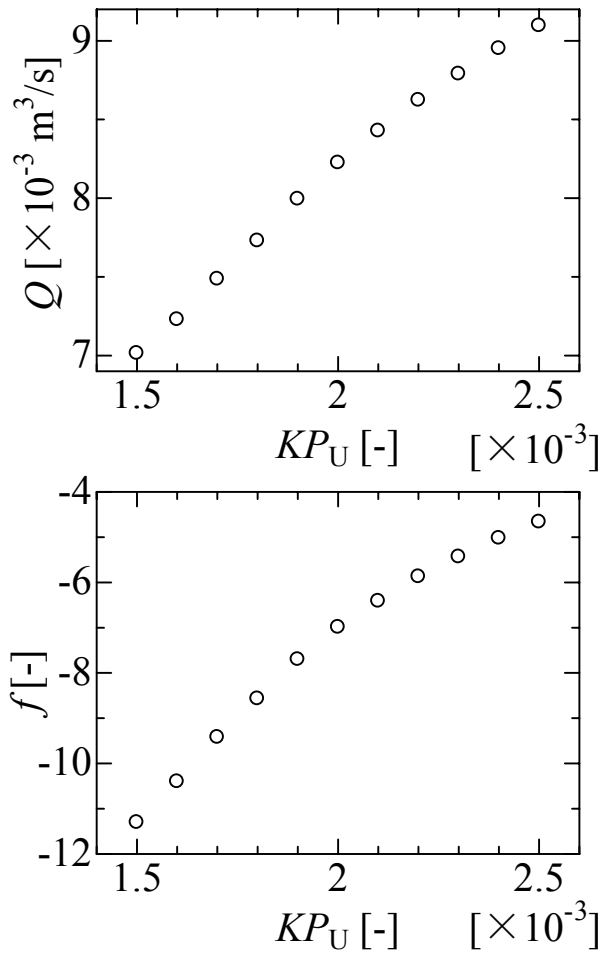

Figure 10. Variation of estimation of Q and feedback signal f against KP_U at first computation time step

same as shown in **Table 1**. When KP_U was increased, estimation of inlet flow rate became larger than actual values, and correction effect of feedback signal f became smaller. This means that computation results depend on convergent speed of the feedback loop.

CONCLUSION

In this study, the developed MI simulation from wall pressure measurement using a turbulent model was evaluated in unsteady sinusoidal oscillating flow passing an orifice plate in a circular pipe.

First, experimental measurements are conducted. Unsteady flow rate up to 10 Hz are generated with unsteady flow rate generator. Wall pressures and a center velocity are measured in each condition. Upstream pressure P_1 and downstream pressure P_2 are used for feedback control.

Then, the developed MI simulation was evaluated by comparing to the experiment. The effectiveness in computation accuracy up to 10 Hz was confirmed when feedback gains were configured adequately. It is clarified that computation results depend on convergent speed of the feedback loop. The problem will be fixed by developing a determination method of feedback gains or adding a new feedback point. They are our future challenge.

REFERENCES

[1] T. Hayase and S. Hayashi, State Estimator of Flow as an Integrated Computational Method with the Feedback of Online Experimental Measurement, Trans. ASME, J. of Fluids Eng., Vol.119, No., pp.814-822, (1997)

[2] K. Funamoto, T. Hayase, A. Shirai, Y. Saijo and T. Yamabe, Fundamental Study of Ultrasonic-Measurement-Integrated Simulation of Real Blood Flow in the Aorta, Annals of Biomedical Engineering, Vol. 33, No. 4, pp.415-428, (2005)

[3] K. Nisugi, T. Hayase and A. Shirai, Fundamental Study of Hybrid Wind Tunnel Integrating Numerical Simulation and Experiment in Analysis of Flow Field, JSME International Journal, Series B, Vol. 47, No. 3, pp.593-604, (2004)

[4] M. Nakao, K. Kawashima and T. Kagawa, Application of MI simulation Using a Turbulent Model for Unsteady Orifice Flow, Trans. ASME J. Fluids Eng., Vol. 131, No. 11, pp. 111401: 1-6 (2009)

[5] M. Nakao, K. Kawashima and T. Kagawa, Visualization of Orifice Flow with Measurement-Integrated Simulation Using a Turbulent Model, Trans. SICE, Vol. 45, No. 12, pp. 671-677, (2009) (in Japanese)

[6] M. Nakao, K. Kawashima and T. Kagawa, Visualization of a steady Orifice Flow in a Circular Pipe from Wall Pressure Measurement Based on Measurement-integrated Simulation Using Turbulent Model, ISFV 14, will be published

[7] W. P. Jones and B. E. Launder, The Numerical Computation of Turbulent Flows, Comp. Method Appl. Mech. Eng., Vol. 3, pp. 269-289, (1974)

[8] A. Erdal and H. I. Anderson, Numerical Aspects of Flow Computation Through Orifices, Flow Meas. Instrum., Vol. 8. No. 1, pp.27-37, (1997)

[9] S. V. Patankar, Numerical Heat Transfer and Fluid, Flow, McGraw-Hill, (1980)

[10] K. Kawashima and T. Kagawa, Unsteady flow generator for gases using isothermal chamber, Measurement, Journal of the International Measurement Confederation (IMEKO), 33-4, pp.333-340, (2003)

[11] T. Funaki, K. Sengoku, K. Kawashima, T. Kagawa, Dynamic Calibration of Laminar Flow Sensor for Gases, SICE Annual Conference, CD-ROM (2004)